JOURNAL OF MATERIALS SCIENCE **34** (1999) 5975–5982

Phase transformations in plasma source ion nitrided austenitic stainless steel at low temperature

M. K. LEI
Surface Engineering Laboratory, Department of Materials Engineering and State Key Laboratory for Materials Modification by Laser, Ion and Electron Beams, Dalian University of Technology, Dalian 116024, People's Republic of China
E-mail: mklei@gingko.dlut.edu.cn

Plasma source ion nitriding has emerged as a low-temperature, low-pressure nitriding approach for low-energy implanting nitrogen ions and then diffusing them into steel and other alloys. In this work, 1Cr18Ni9Ti (18-8 type) austenitic stainless steel was treated at a process temperature from 280 to 480 °C under an average nitrogen implantation dose rate (nitrogen ion current density) of 0.44–0.63 mA cm^{-2} during a nitriding period of 4 h. The nitrided surfaces of the stainless steel were characterized using Auger electron spectroscopy, electron probe microanalysis, glancing angle X-ray diffraction, and transmission electron microscopy. Below 300 °C, a high nitrogen f.c.c. phase (γ_N) and an ordered f.c.c. phase (γ') mixed phase and a γ_N and a nitrogen-induced martensite (ε'_N) mixed phase were obtained respectively under lower and higher nitrogen implantation dose rates. In the range of 300–450 °C a single γ_N phase was observed under various nitrogen implantation dose rates. Above 450 °C, the decomposition of the γ_N phase to a CrN phase with a b.c.c. martensite was obtained. Phase states and phase transformations in the plasma source ion nitrided 1Cr18Ni9Ti stainless steel at the low process temperatures are dependent on all the process parameters, including process temperature, nitrogen implantation dose rate, nitrogen ion energy, and processing time, etc.. The process parameters have significant effects on the formation and transformation of the various phases.

1. Introduction

Phase states and phase transformations in the nitrogen-modified 18-8 type austenitic stainless steels at low process temperatures in the range of 200–500 °C by low-temperature nitriding [1–9], nitrogen ion beam implantation [10–12], or nitrogen plasma immersion ion implantation (PIII) [13–15] have been investigated in order to improve the combined wear and corrosion resistance of the stainless steels over the last twenty years. In most studies, a new phase, which stems from supersaturation of nitrogen in austenite (γ) matrix, was obtained on the nitrogen-modified surfaces by three processes. The anisotropic distribution of disordered nitrogen ranging from about 10 to 35 at % in f.c.c. lattice of the γ matrix resulted in a complicated structure of the new phase. Its X-ray diffraction pattern showed a set of broad peaks which appear to the low 2θ angles side of each austenite peak for the γ matrix. The intensity and position shift of the each broad peak also changed with varying nitrogen concentration on the nitrogen-modified layer with various thicknesses, and some peaks of high-index planes may completely disappear. On the basis of X-ray diffraction data, the different types of structure were defined for the new phase. Zhang and Bell [1] reported that a nitrogen-supersaturated austenite formed in plasma-nitrided AISI 316 stainless steel. Ichii *et al.* [2] described the phase as a ferro-magnetic Fe_4N-like phase, called "S" phase, in ion-nitrided 18-8 type stainless steel. Williamson *et al.* [12] called the phase "a high nitrogen f.c.c. phase (γ_N)", and summarized the formation conditions of the γ_N phase on the nitrogen-modified surfaces of 18-8 type stainless steels. Marchev *et al.* [9] reported the microstructure of a phase similar to that of the γ_N phase in low-temperature ion nitrided 300 series (18-8 type) stainless steels and affirmed it as a b.c.t. martensite phase. Furthermore, other phases also were obtained on the nitrogen-modified surfaces at the low process temperatures. Hannula *et al.* [3] showed that low-temperature plasma nitriding into SS2333 and SS2343 (18-8 type) stainless steels at 350 °C formed an h.c.p. nitride in the γ_N phase matrix, which is different from ε-Fe_2N_{1-x} ($0 \leq x \leq 1/3$) nitride [16] and analogous to h.c.p. martensite [17]. The $(Cr, Fe)_2N_{1-x}$ nitride was observed in plasma nitrided AISI 304 stainless steel at 400–450 °C by D'Haen *et al.* [5]. Leutenecker *et al.* [10] found that the b.c.c. and/or h.c.p. martensites could form in the γ_N phase matrix in nitrogen ion

implanted X10CrNiTi18-9 (18-8 type) stainless steel at 350 °C.

In addition, some of mechanical and chemical properties for the γ_N phase reported in the three processes mentioned above are often different. The microhardness of the γ_N phase was varied over a large range of about HV 1000–2000 [2, 8, 12]. The general corrosion resistance in a H_2SO_4 solution was even conflicting [6, 8, 14]. The difference of the properties of the γ_N phase may be attributed to the complex phase states and their different microstructures on the nitrogen-modified surfaces of the stainless steels. In spite of extensive studies of the nitrogen-modified 18-8 type stainless steels at low process temperatures, little is known about the formation mechanisms of the nitrogen-containing relative phases, such as γ_N, h.c.p. nitride, b.c.c. and/or h.c.p. martensites etc., in the stainless steels. The formation conditions of the phases also are not fully understood.

Plasma source ion nitriding has emerged as a new low-temperature, low-pressure nitriding approach combining low-energy nitrogen ion implantation and implanted nitrogen diffusion into steel and alloy [18, 19]. It enables independent measurements and control of nitrogen ion energy, nitrogen implantation dose rate (ion current density), and process temperature, thereby providing additional possibilities for investigation of formation and transformation of the phases in the nitrided stainless steels at low process temperatures. We have found that a single γ_N phase was obtained in the plasma source ion nitrided 1Cr18Ni9Ti (18-8 type) austenitic stainless steel in the range of 300–450 °C, the ordering of the γ_N phase to a γ'-$(Fe,Cr,Ni)_4N$ phase carried out below 300 °C, and the precipitation of CrN phase in the γ_N phase matrix occurred above 450 °C [18, 20]. The γ_N, γ', and CrN phases were observed in the nitriding process under a lower nitrogen implantation dose rate. With increasing nitrogen implantation dose rate, a nitrogen-induced h.c.p. martensite (ε'_N) was obtained on the nitrided surface below 300 °C [21]. During the nitriding process the ε'_N martensite later transformed to a disordered nitrogen-containing h.c.p. phase (ε_N) [22]. The transformation of γ_N phase in the nitrided 1Cr18Ni9Ti stainless steels is obviously dependent on the nitrogen implantation dose rate except for the process temperature and nitriding time. In this article, the effects of the process parameters on formation and transformation of the nitrogen-containing phases were systemically investigated using Auger electron spectroscopy (AES), electron probe microanalyser (EPMA), X-ray diffraction and transmission electron microscopy (TEM) in order to explore the formation mechanisms of the phases in the nitrogen-modified stainless steels at low process temperatures.

2. Experimental

2.1. Sample preparation

Commercial 1Cr18Ni9Ti austenitic stainless steel was selected as the test material. Its composition (wt %) was C 0.10, Mn 1.50, Si 0.80, Cr 18.00, Ni 9.00, Ti 0.80, $P \leq 0.035$, $S \leq 0.030$ and Fe as the balance. Samples (25 mm diameter $\times$6 mm length) were cut from bars of the stainless steel in the hot rolled condition. All samples were finely ground through 180, 400 and 800 grit silicon carbide paper, polished using 1 μm diamond paste, and finally cleaned in acetone followed by air drying.

TABLE I Typical ECR microwave plasma source ion nitriding parameters

Microwave power	300 W
Density of nitrogen plasma	5×10^{11}–1.5×10^{12} cm^{-3}
Electron temperature of nitrogen plasma	7–10 eV
Base pressure	1.5×10^{-3} Pa
Nitriding pressure	$(5–10) \times 10^{-2}$ Pa
Pulsed negative bias	
Voltage	−2.0 kV
Repetition rate	100–1000 Hz
Length	50–500 μs
Nitrogen implantation dose rate	0.44–0.63 mA cm^{-2}
Process temperature	280–480 °C
Nitriding time	4 h

2.2. Plasma source ion nitriding process

In the plasma source ion nitriding process, samples were placed in an electron cyclotron resonance (ECR) microwave plasma and biased with a pulsed negative potential of −2 kV at a process temperature of 280–480 °C regulated by an auxiliary heater. The sample temperatures were always measured during the nitriding process by a thermocouple attached within 2 mm of the surface being nitrided. The nitrogen ion implantation dose rates (average nitrogen ion current density) of 0.44 and 0.63 mA cm^{-2} were selected for the nitriding process during a nitriding period of 4 h. The plasma source ion nitriding device, which is described elsewhere [18], was pumped down to a base pressure of 1.5×10^{-3} Pa by a diffusional/mechanical pump package. The typical operating parameters applied during the nitriding process are listed in Table I.

2.3. Characterization of nitrided samples

The nitrogen concentration profile of the nitrided surfaces was made to a depth of 400 nm by Auger electron spectroscopy (AES) using a RIBER SIA-100 surface analysis system and to a depth of 50 μm using a JXA-733 electron probe microanalyser (EPMA). The AES gives good depth resolution while the EPMA provides semiquantitative compositional profiles to considerably great depths. The near-surface structure of the nitrided samples was investigated using glancing angle X-ray diffraction on a Rigaku D/Max-3A diffractometer using Cu K_α radiation. An incidence angle of 10° was used for all samples. The microstructural characteristics of the nitrided layer were also investigated using JEOL-100CX and Hitachi-800 transmission electron microscopes (TEM). TEM foils from the outer surface region of the nitrided samples were prepared by cutting and grinding them to a thickness of 0.08–0.10 mm, subsequently being single ion beam thinned before insertion into the electron microscope.

3. Experimental results

3.1. Nitriding below 300 °C

Fig. 1 shows the nitrogen concentration depth profiles by AES and EPMA on the nitrided surfaces of the stainless steel at a process temperature of 280 °C. Nitriding under a lower nitrogen implantation dose rate of 0.44 mA cm^{-2} yielded a nitrogen concentration layer with a peak nitrogen concentration of about 22 at %. The thickness of the nitrided layer was approximately 1 μm. Under a higher nitrogen implantation dose rate of 0.63 mA cm^{-2}, the peak nitrogen concentration of the nitrided layer increased to about 32 at % and the nitrogen penetration depth increased by five times to about 5 μm.

The crystal structure and lattice parameter of the nitrided layers at 280 °C were investigated using X-ray diffraction, as shown in Fig. 2. In the nitriding process below 300 °C, the predominant peaks of γ phase resulted from the stainless steel matrix due to the thin nitrided layers. An ordered γ' and a γ_N mixed phase was obtained on the nitrided surface under 0.44 mA cm^{-2}. For the thicker nitrided layer under 0.63 mA cm^{-2}, the diffraction peaks of the γ_N phase showed a typical pattern of an f.c.c. lattice, although its lattice parameter was difficulty determined due to apparently broadening of the peaks caused by the gradient nitrogen concentration depth profiles on the nitrided surfaces. A new h.c.p. phase was also obtained in the γ_N phase matrix. Considering the formation of the h.c.p. phase should be in a well-distributed nitrogen concentration zone of the γ_N phase, the lattice constants of the h.c.p. phase were estimated using X-ray diffraction pattern, $a = 0.280$ nm, $c = 0.456$ nm and $c/a = 1.63$. More detailed studies of the nitrided layers using TEM have clearly demonstrated that the outermost surface microstructures are consistent with those detected using X-ray diffraction, as shown in Figs 3 and 4. Fig. 3a shows that a typical area of γ' phase in the γ_N phase matrix on the nitrided surface under 0.44 mA cm^{-2}. The stacking faults were observed both in the γ_N phase and in the γ' phase. The selected area diffraction (SAD) patterns from the γ_N phase and the γ' phase are presented in Fig. 3 b–d, respectively. Fig. 3b and c show a [001] zone and a [011] zone of an f.c.c. lattice. The SAD patterns indicate unambiguously that the γ_N phase has an f.c.c. structure and the nitrogen is disordered distribution in the f.c.c. lattice. Compared with the γ_N phase, the γ' phase has an ordered f.c.c. structure according to the presence of a [011] f.c.c. zone with superlattice spots (Fig. 3d). Fig. 4a shows the blocks of platelike features on the nitrided surface under 0.63 mA cm^{-2}. The SAD pattern shows clearly the existence of an h.c.p. zone and an f.c.c. zone (Fig. 4b), corresponding to the presence of an h.c.p. phase, denoted by ε'_N, together with a γ_N phase. The lattice constants of the ε'_N phase are consistent with those detected by X-ray diffraction (Fig. 2). The diffraction pattern was indexed as [251] γ_N and [$\bar{2}\bar{4}23$] ε'_N. The two phases have exactly the same orientation. The γ_N/ε'_N orientation relationship was found to be (111) γ_N//(0001) ε'_N, [011] γ_N//[1210] ε'_N.

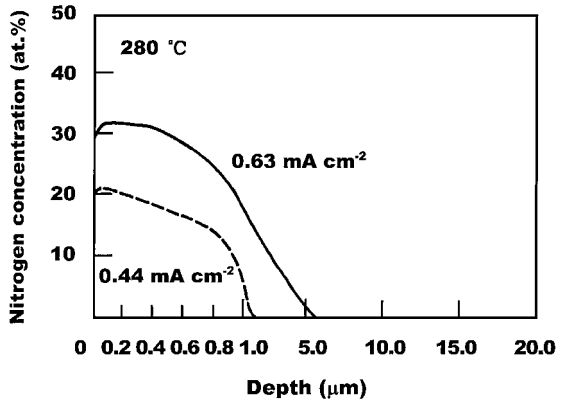

Figure 1 AES and EPMA depth profile of nitrogen in the 1Cr18Ni9Ti stainless steel nitrided at 280 °C under various nitrogen implantation dose rates.

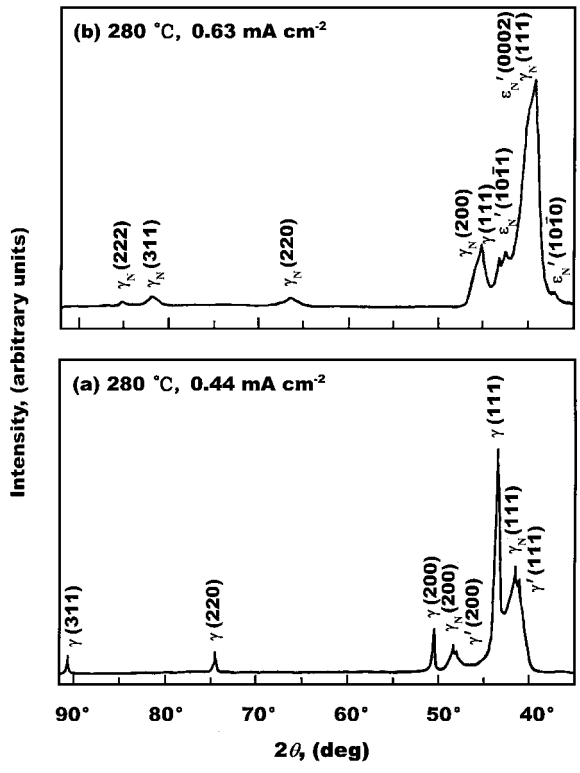

Figure 2 Glancing X-ray diffractograms of the 1Cr18Ni9Ti stainless steel nitrided at 280 °C under various nitrogen implantation dose rates. (a) 0.44 mA cm^{-2}; (b) 0.63 mA cm^{-2}.

3.2. Nitriding in the range of 300–450 °C

Fig. 5 shows the AES and EPMA depth profiles of nitrogen on the nitrided samples at 380 °C. The peak nitrogen concentration of the nitrided layers under 0.44 and 0.63 mA cm^{-2} was about 26 and 32 at %, respectively. Nitriding in the range of 300–450 °C resulted in the thicker nitrided layers. The thicknesses of about 12 and 13 μm were respectively for the nitrided samples under the two nitrogen implantation dose rates. The increase of thickness of the nitrided layers did not be apparently affected by the nitrogen implantation dose rate.

Fig. 6 shows that a single γ_N phase on the nitrided surfaces at 380 °C under the two nitrogen implantation dose rates was detected by X-ray diffraction. Changes in the intensity and position of peaks of the γ_N phase are associated with the higher peak nitrogen concentrations

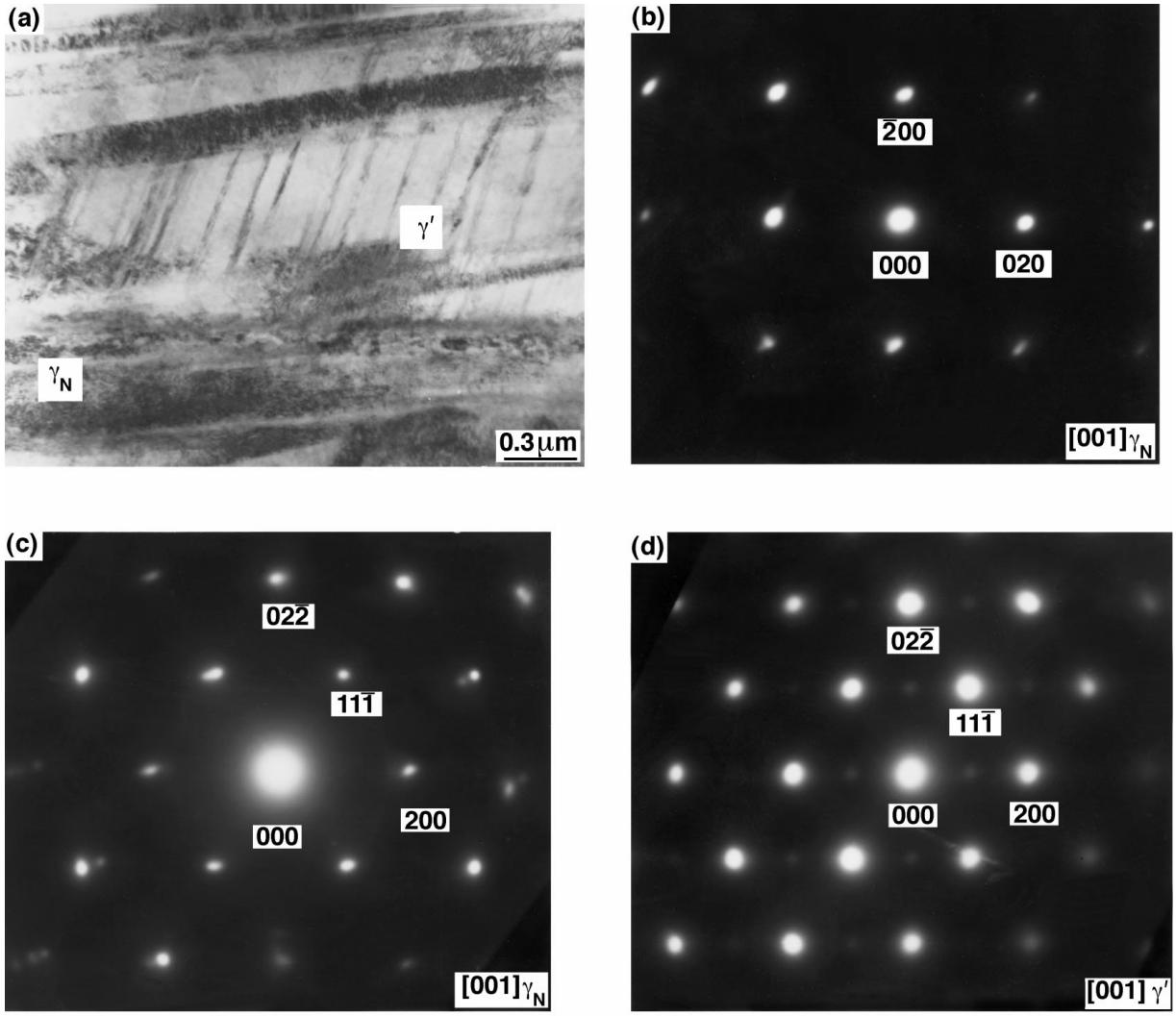

Figure 3 TEM images of the outer surface layer of the 1Cr18Ni9Ti stainless steel nitrided at 280 °C under a nitrogen implantation dose rate of 0.44 mA cm^{-2}: (a) Bright field micrograph; (b) selected area diffraction pattern of the γ_N phase showing [001] zone; (c) selected area diffraction pattern of the γ_N phase showing [011] zone; (d) selected area diffraction pattern of the γ' phase showing [011] zone.

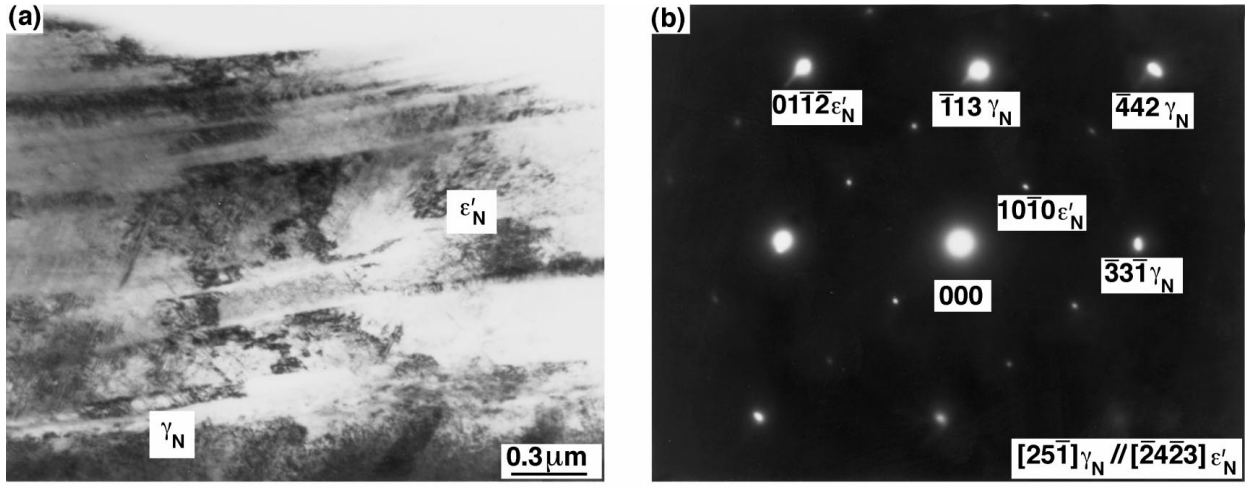

Figure 4 TEM images of the outer surface layer of the 1Cr18Ni9Ti stainless steel nitrided at 280 °C under a nitrogen implantation dose rate of 0.63 mA cm^{-2}: (a) Bright field micrograph; (b) selected area diffraction pattern, showing $[25\bar{1}]\gamma_N$ zone and $[\bar{2}4\bar{2}3]\varepsilon'_N$ zone.

on the thicker nitrided layers. With increasing peak nitrogen concentration of the γ_N phase, the expansion of f.c.c. lattice leads to further shift of the peaks to lower 2θ angle and completely disappearing the distinct peak of high-index (222) plane. The formation of a single γ_N phase on the two nitrided surfaces has also been confirmed unambiguously by TEM observation, as shown in Figs 7 and 8. The stacking faults and dislocations were a result of great strain in the f.c.c. lattice from the high nitrogen supersaturation for the

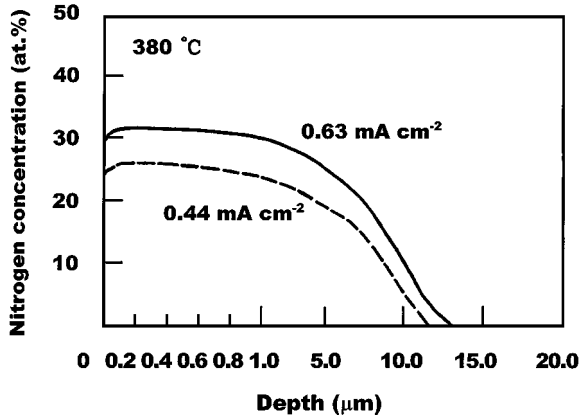

Figure 5 AES and EPMA depth profile of nitrogen in the 1Cr18Ni9Ti stainless steel nitrided at 380 °C under various nitrogen implantation dose rates.

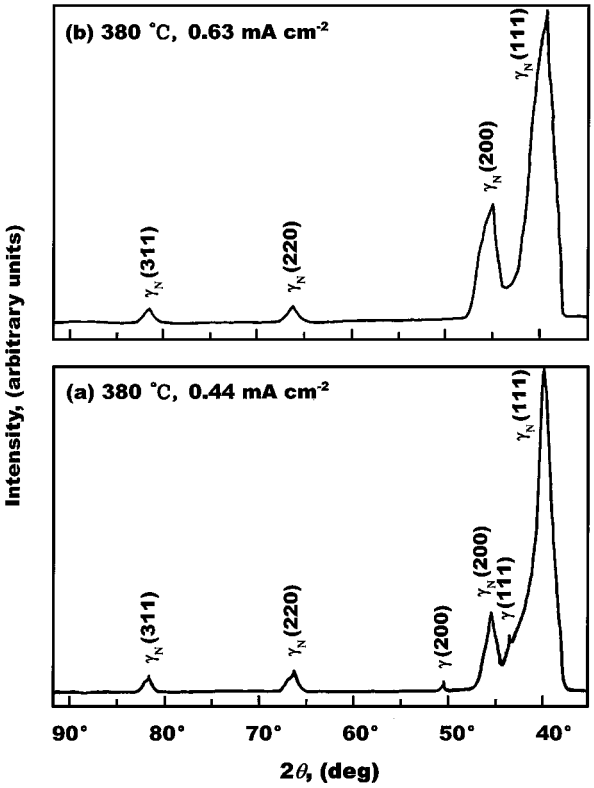

Figure 6 Glancing X-ray diffractograms of the 1Cr18Ni9Ti stainless steel nitrided at 380 °C under various nitrogen implantation dose rates. (a) 0.44 mA cm^{-2}; (b) 0.63 mA cm^{-2}.

two samples [Fig. 7a and 8a]. The dense and wide microstructure suggested a very low nucleation rate of the γ_N phase. The electron diffraction patterns of the γ_N phases are similar to those obtained on the nitrided layers at 280 °C. Figs 7b and 8b showed a single γ_N phase with a $[\bar{1}12]$ zone and a $[\bar{2}51]$ zone on the nitrided surfaces under the two nitrogen implantation dose rates, respectively. The TEMs have shown that the nitriding in the range of 300–450 °C produced a single γ_N phase layer on the nitrided surfaces, which is completely free of nitrides (e.g. nitrides of chromium, iron, etc.).

3.3. Nitriding above 450 °C

Fig. 9 shows the AES and EPMA depth profiles of nitrogen on the nitrided samples at 480 °C. Nitriding under the two nitrogen implantation dose rates yielded the similar peak nitrogen concentrations, 25 at % and 26 at %, and thicknesses, both about 17 μm. Above 450 °C, no effects of the nitrogen implantation dose rate on the nitrogen penetration depth were observed obviously.

Fig. 10 shows that the signs of γ_N, b.c.c. martensite, and CrN phases on the nitrided surfaces under the two nitrogen implantation dose rates detected by X-ray diffraction. At 480 °C, the peaks of the γ_N phase shifted to higher 2θ angle than those for the nitrided samples in the range of 300–450 °C. For the two nitrided samples the precipitation of CrN phase was accompanied by decomposition of the γ_N phase to b.c.c. martensite during the nitriding process.

4. Discussion

4.1. Formation conditions of γ_N phase

The formation of γ_N phase which is called an expanded austenite initially was reported in the nitrogen ion implanted AISI 304 stainless steel by Singer and co-workers [23]. The nitrogen ion implantation into the stainless steel led to the transformation of strain-induced b.c.c. martensite formed on the polished surfaces of metastable stainless steel to the γ_N phase. It is significant that the engineering surfaces composed of the γ_N phase called nitrogen-supersaturated austenite primarily was obtained in low-temperature plasma nitrided AISI 316 stainless steel for combined improvement in wear and corrosion resistance by Zhang and Bell [1]. Williamson *et al.* [12] summarized the formation conditions of the γ_N phase in the nitrogen-modified stainless steels. The γ_N phase is often produced in the f.c.c. Cr-containing stainless steels by low-temperature nitriding [1–4, 6, 8], nitrogen ion beam implantation [10–12], or nitrogen PIII [13–15], which provided that appropriate process temperatures and processing times are used. Menthe *et al.* [8] found that the γ_N phase can also form in DIN 1.4460 austeno-ferrite duplex stainless steel (wt %: C 0.1, Cr 26.7, Ni 4.5, Fe as the balance), but it can not form in DIN 1.3917 (wt %: C 0.04, Cr 0.01, Ni 42.1, Fe as the balance) austenitic stainless steel in pulsed plasma nitriding process at 450 °C. The formation of the γ_N phase is independent of the original structures of the nitrogen-modified stainless steels.

Considering the composition condition of the nitrogen-modified stainless steels for formation of the γ_N phase, all the stainless steels reported consist of Cr and Ni elements in base Fe alloy. More recently, Williamson *et al.* [24] showed that the γ_N phase was observed in nitrogen ion implanted Cr-free austenitic alloy (wt %: C + Mn + Si 1.0, Ni 34.0, Fe as the balance), before this, they did not obtain the γ_N phase on nitrogen ion implanted another Cr-free austenitic alloy (wt %: Ni 80.0, Fe as the balance) [25, 12]. In the plasma source ion nitriding process, a series of the Fe-Mn austenitic alloys [26] was treated at 380 °C under same process parameters as those in Table I. The X-ray diffraction patterns of the nitrided Fe-30Mn alloy (wt %: C 0.3, Mn 29.6, Fe as the balance) showed the signs of γ'-$(Fe,Mn)_4N$ and ε-$(Fe,Mn)_2N$ phases, although no

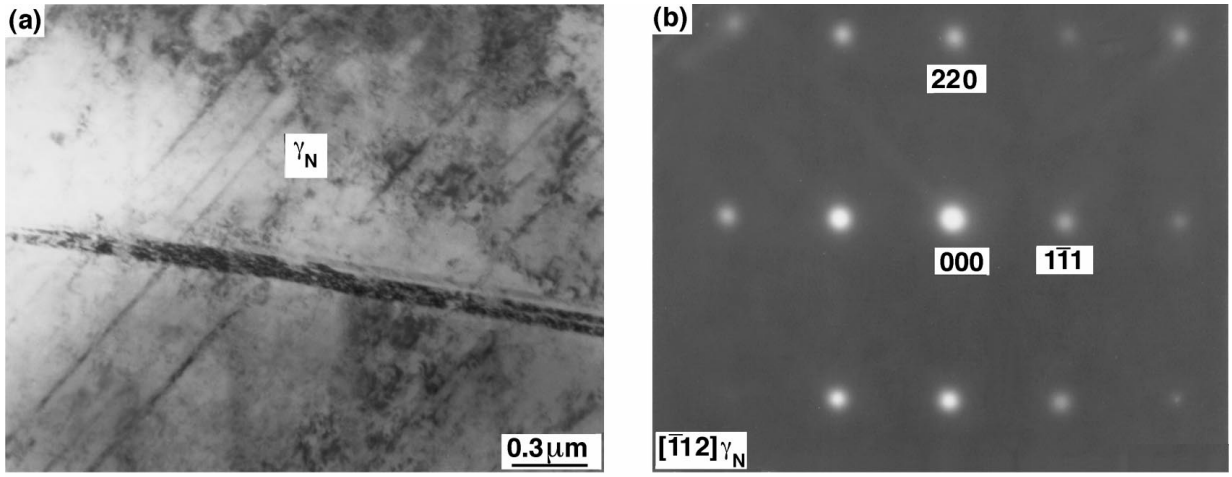

Figure 7 TEM images of the outer surface layer of the 1Cr18Ni9Ti stainless steel nitrided at 380 °C under a nitrogen implantation dose rate of 0.44 mA cm^{-2}: (a) Bright field micrograph; (b) selected area diffraction pattern of the γ_N phase showing $[\bar{1}12]$ zone.

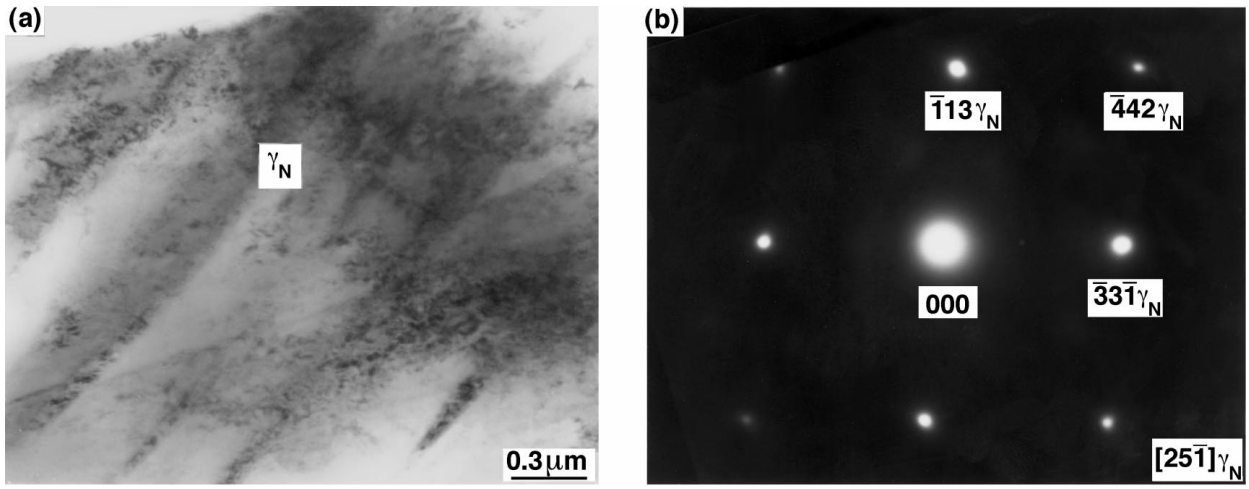

Figure 8 TEM images of the outer surface layer of the 1Cr18Ni9Ti stainless steel nitrided at 380 °C under a nitrogen implantation dose rate of 0.63 mA cm^{-2}: (a) Bright field micrograph; (b) selected area diffraction pattern of the γ_N phase showing $[25\bar{1}]$ zone.

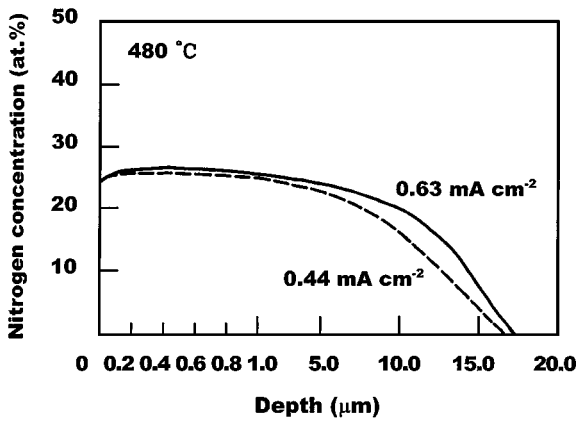

Figure 9 AES and EPMA depth profile of nitrogen in the 1Cr18Ni9Ti stainless steel nitrided at 480 °C under various nitrogen implantation dose rates.

peak of superlattice of γ'-$(Fe,Mn)_4N$ phase was observed. The unambiguous confirmation of formation of γ'-$(Fe,Mn)_4N$ and ε-$(Fe,Mn)_2N$ phases should be made by TEM, work currently in progress. In spite of lack of systemic study on the composition condition, we can speculate that the contents of Cr and Ni and their ratio in the stainless steels play an important role in the formation of the γ_N phase on the nitrogen-modified surfaces.

The plasma source ion nitriding process produced a single γ_N phase with high peak nitrogen concentrations on the nitrided surfaces of 18-8 type stainless steel in the range of 300–450 °C. It also seems to identify that both the process temperature and processing time are the principal process parameters which the formation of the γ_N phase depends on. Below 300 °C the transformation from the γ_N phase to γ' or ε'_N phase carried out on the nitrided surfaces under 0.44 and 0.63 mA cm^{-2}, respectively. This means that the presence of the γ_N phase at lower process temperatures also depends on the other parameters, such as nitrogen implantation dose rate etc. Zhang and Bell [1] reported that a γ' and a γ_N mixed phase was observed on plasma nitrided 18-8 type stainless steel at 400 °C. Hannula *et al.* [3] showed both γ' and ε'_N phases in the γ_N phase formed on the nitrided 18-8 type stainless steels at 350 °C. In different nitrogen-modified processes, the upper limit of process temperature for transformation of $\gamma_N \rightarrow \gamma'$ or $\gamma_N \rightarrow \varepsilon'_N$ was varied in the range of 200–400 °C. Above 450 °C, the CrN phase and b.c.c. martensite were obtained on the nitrided surfaces. The prevention

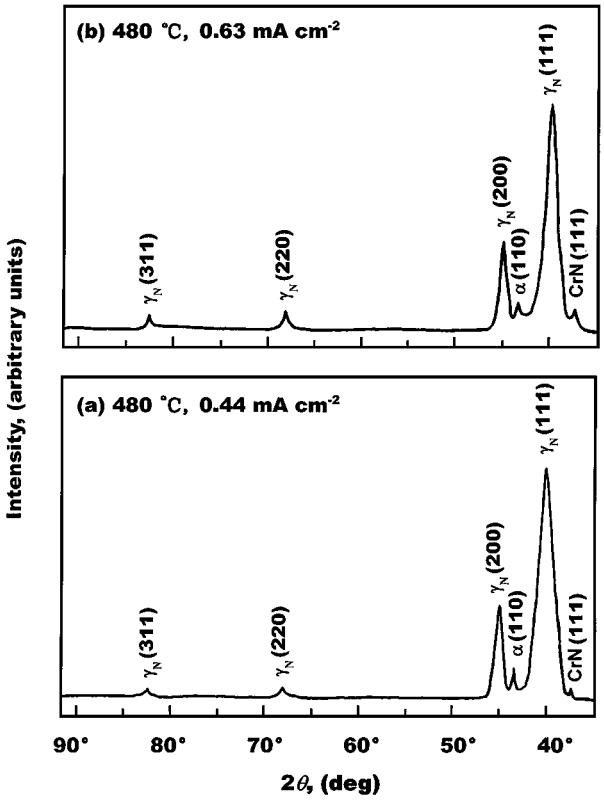

Figure 10 Glancing X-ray diffractograms of the 1Cr18Ni9Ti stainless steel nitrided at 480 °C under various nitrogen implantation dose rates. (a) 0.44 mA cm^{-2}; (b) 0.63 mA cm^{-2}.

of long-range diffusion of Cr, Ni atoms in nitrogen-supersaturated f.c.c. lattice below a critical temperature of about 500 °C could assure the presence of the γ_N phase. The lower limit of process temperature for decomposition of the γ_N phase to CrN phase also scattered over a larger range from 450 to 600 °C [1, 12, 14, 18]. Therefore, the process parameters including the process temperature, nitrogen implantation dose rate, nitrogen ion energy, and processing time, etc. jointly affect the formation and transformation of the γ_N phase in the nitrogen-modified stainless steels by the various nitrogen-modified processes.

4.2. Formation conditions of ε'_N martensite

Compared with the strain-induced and hydrogen-induced h.c.p. martensites [17, 27], the ε'_N phase is a nitrogen-induced h.c.p. martensite, which has been shown to be crystallographically identical to the strain-induced h.c.p. martensite. The transformation from the γ_N phase to ε'_N martensite was by a faulting mechanism from ABCABC... (f.c.c.) to ABABAB... (h.c.p.) according to Olson and Cohen [28]. At lower process temperatures the formation of the ε'_N martensite from the γ_N phase took place on the nitrided surface with a gradient nitrogen concentration exceeding a threshold of peak nitrogen concentration, below which ordering of the γ_N phase to the γ' phase will occur. The stress condition caused by the gradient nitrogen concentration decides the formation of either ε'_N martensite or γ' phase on the nitrogen-modified surfaces. We believe that the transformation from the γ_N phase to the ε'_N martensite achieved by the strain-induce mechanism. The high stress on the nitrided surfaces led to the transformation, although the solution of nitrogen in the γ phase matrix increased the stacking fault energy. The formation mechanism of the ε'_N martensite is similar to that of stain-induced h.c.p. martensite, however, it is different with that of hydrogen-induced h.c.p. martensites because the hydrogen supersaturation decreasing the stacking fault energy caused the fault movement to form the h.c.p. martensite [27].

The nitrogen-induced h.c.p. martensite, ε'_N, was obtained in the plasma source ion nitrided 18-8 type stainless steel, following the formation of strain-induced and hydrogen-induced h.c.p. martensites in the stainless steels [17, 27]. Owing to complex vacuum technologies and processes without independent control of nitrogen ion energy, nitrogen implantation dose rate and/or process temperature, it is very difficult to determine the characteristics of ε'_N martensite. Low-temperature plasma nitriding of 18-8 type stainless steels also produced the ε'_N martensite, albeit a smaller amount was obtained at higher process temperatures [3]. Despite more complex effects of high-energy (about 40–100 keV) ion bombardment on the microstructure and temperature of the surfaces in nitrogen ion implantation process, the ε'_N martensite formed under a proper nitrogen ion implantation dose rate at a given process temperature [10, 29]. Because the ε'_N martensite is produced by strain-induced mechanism at lower process temperatures, the nitrogen implantation dose rate is a more important parameter among the process parameters in comparison with that for formation of the γ_N phase.

4.3. Phase diagram of nitrided austenitic stainless steel

On the basis of the discussion described in 4.1 and 4.2, a phase diagram for the plasma source ion nitrided 1Cr18Ni9Ti stainless steel in the range from 200–500 °C is illustrated in Fig. 11. In the phase diagram the formation of the nitrogen-containing relative phases, γ_N, ε'_N, CrN, and α' etc., depending on the peak nitrogen concentration and process temperature

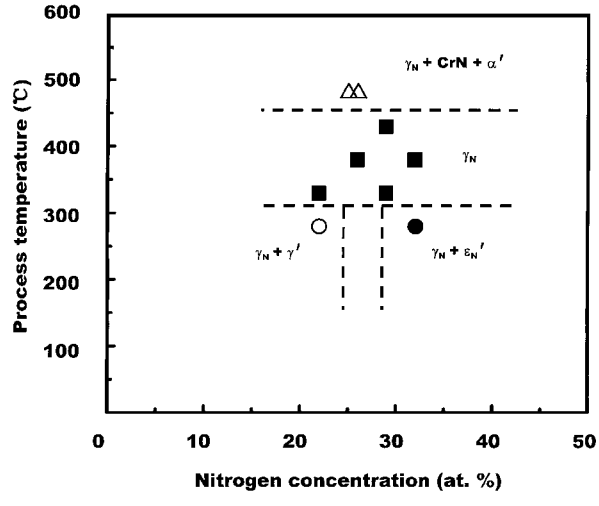

Figure 11 Phase diagram for the plasma source ion nitrided 1Cr18Ni9Ti stainless steels in the range from 200 to 500 °C.

was reviewed in order to take in consideration of effects of process parameters except for the process temperature. The peak nitrogen concentration of the single γ_N phase on the nitrided surfaces at 330 and 430 °C was also measured respectively by AES. Although accurate phase boundaries could not be defined in the phase diagram, it does give the formation conditions of the phases and the possibility of formation of other relative phases, and predict the presence of other phase regions, such as single phase, biphase equilibrium, and/or triphase equilibrium regions. Most nitrogen-modified processes for 18-8 type stainless steels at low process temperatures in the range of 200–500 °C completely or partly comply with patterns of the phase region diagram [1, 12, 14, 15]. The differences between the patterns are caused by the jointly effects of different process parameters, including the process temperature, nitrogen implantation dose rate, nitrogen ion energy, and processing time, etc., in the various nitrogen-modified processes.

5. Conclusions

(1) Plasma source ion nitriding into 1Cr18Ni9Ti austenitic stainless steel below 300 °C formed two type mixing phases: a high nitrogen f.c.c. phase (γ_N) and an ordered f.c.c. phase (γ') mixed phase under a low nitrogen implantation dose rate of 0.44 mA cm^{-2} and a γ_N and a nitrogen-induced martensite (ε'_N) mixed phase under a high nitrogen implantation dose rate of 0.63 mA cm^{-2}.

(2) Plasma source ion nitridng into 1Cr18Ni9Ti stainless steel in the range of 300–450 °C produced a single γ_N phase, which is completely free of nitrides (e.g. nitrides of chromium, iron, etc.), under the various nitrogen implantation dose rates.

(3) Plasma source ion nitriding into 1Cr18Ni9Ti stainless steel above 450 °C the γ_N phase decomposed to a CrN phase together with a b.c.c. martensite. The higher process temperatures lead to a decrease in the peak nitrogen concentration and increase the nitrogen penetration depth.

(4) Phase states and phase transformations in the plasma source ion nitrided 1Cr18Ni9Ti stainless steel at the low process temperatures are dependent on all the process parameters, such as process temperature, nitrogen implantation dose rate (nitrogen ion current density), nitrogen ion energy, and processing time, etc.. The process parameters have significant effects on the formation and transformation of the various phases.

Acknowledgements

The author is very grateful to Professor Z. L. Zhang, Dr. Y. Huang, Professor Z. K. Hei, and Mrs. X. L. Xu and L. J. Yuan for their contributory discussions and technical assistance. This work is supported by the National Science Foundation of China under Grant No. 59771060.

References

1. Z. L. ZHANG and T. BELL, *Surf. Eng.* **1** (1985) 131.
2. K. ICHII, K. FUJIMARA and T. TAKASE, *Rep. Kansai Univ.* **27** (1986) 135.
3. S.-P. HANNULA, P. NENONEN and J. P. HIRVONEN, *Thin Solid Films* **181** (1989) 343.
4. K. GEMMA and M. KAWAKAMI, *High Temp. Mater. Proc.* **8** (1989) 205.
5. J. D'HAEN, C. QUAEYHAEGENS, G. KNUYT, L. DE SCHEPPER, L. M. STALS and M. VAN STAPPEN, *Surf. Coat. Technol.* **60** (1993) 468.
6. N. YASUMARU, K. TSUCHIDA, E. SAJI and T. IBE, *Mater. Trans. JIM* **34** (1993) 696.
7. E. I. MELEIIS and S. YAN, *J. Vac. Sci. Technol.* **A 11** (1993) 25.
8. E. MENTHE, K.-T. RIE, J. W. SCHULZE and S. SIMSON, *Surf. Coat. Technol.* **74/75** (1995) 412.
9. K. MARCHEV, C. V. COOPER, J. T. BLUCHER and B. C. GIESSEN, *ibid.* **99** (1998) 225.
10. R. LEUTENECKER, G. WANG, T. LOUIS, U. GONSER, L. GUZMAN and A. MOLINARI, *Mater. Sci. Eng.* **A 115** (1989) 229.
11. D. L. WILLIAMSON, L. WANG, R. WEI and P. J. WILBUR, *Mater. Lett.* **9** (1990) 302.
12. D. L. WILLIAMSON, O. OZTURK, R. WEI and P. J. WILBUR, *Surf. Coat. Technol.* **65** (1994) 15.
13. G. A. COLLINS, R. HUTCHINGS and J. TENDYS, *Mater. Sci. Eng.* **A 139** (1991) 171.
14. M. SAMANDI, A. PAUZA, G. HATZIANDONIOU, H. YASBANDHA, R. HUTCHINGS, G. A. COLLINS and J. TENDYS, *Surf. Coat. Technol.* **54/55** (1992) 447.
15. M. SAMANDI, B. A. SHEDDEN, D. I. SMITH, T. BELL, G. A. COLLINS, R. HUTCHINGS and J. TENDYS, *J. Vac. Sci. Technol.* **B 12** (1994) 935.
16. D. GEARDIN, H. MICHEL, J. P. MORNIROLI and M. GANTOIS, *Mem. Sci. Rev. Metall.* **74** (1977) 457.
17. J. DASH and H. M. OTTE, *Acta. Metall.* **11** (1963) 1169.
18. M. K. LEI and Z. L. ZHANG, *J. Vac. Sci. Technol.* **A 13** (1995) 2986.
19. *Idem., Surf. Coat. Technol.* **91** (1997) 25.
20. *Idem., J. Vac. Sci. Technol.* **A 15** (1997) 421.
21. *Idem., J. Mater. Sci. Lett.* **16** (1997) 1567.
22. M. K. LEI, Y. HUANG and Z. L. ZHANG, *ibid.* **17** (1998) 1165.
23. I. L. SINGER, *Appl. Surf. Sci.* **18** (1984) 28.
24. D. L. WILLIAMSON, J. A. DAVIS and P. J. WILBUR, *Surf. Coat. Technol.* **103/104** (1998) 178.
25. D. L. WILLIAMSON, I. IVANOV, R. WEI and P. J. WILBUR, *Mater. Res. Soc. Symp. Proc.* **235** (1992) 473.
26. X. M. ZHU and Y. S. ZHANG, *Corrosion* **54** (1998) 3.
27. H. L. HOLZWORTH and M. R. LOUTHAN, *ibid.* **24** (1968) 110.
28. G. B. OLSON and M. COHEN, *Metall. Trans.* **A 7** (1976) 1897.
29. S. FEYEULLE, D. TREHEUX and C. ESNOUF, *Appl. Surf. Sci.* **25** (1986) 288.

Received 18 February
and accepted 21 June 1999